

[文章编号] 1671-587X(2025)06-1475-12

DOI:10.13481/j.1671-587X.20250604

针刺对膝骨关节炎模型大鼠股四头肌卫星细胞分化和凋亡的影响及其机制

郑曲^{1,2,3}, 董宝强^{1,3}, 林星星^{1,3}, 张宇¹, 关雪峰⁴, 王超杰¹, 韩易言¹

(1. 辽宁中医药大学针灸推拿学院, 辽宁 沈阳 110847; 2. 辽宁省教育厅针灸生物学重点实验室, 辽宁 沈阳 110847; 3. 辽宁省针灸养生康复重点实验室, 辽宁 沈阳 110847; 4. 沈阳药科大学, 辽宁 沈阳 110016)

[摘要] **目的:** 探讨针刺对膝骨关节炎(KOA)模型大鼠股四头肌卫星细胞分化和凋亡的影响, 并阐明其相关机制。**方法:** 选取40只SPF级大鼠随机分为对照组、模型组、塞来昔布组和针刺组, 每组10只。对照组大鼠仅切开关节腔后缝合, 模型组、塞来昔布组和针刺组大鼠复制KOA模型。测量各组大鼠患肢股骨段最大周长、大鼠体质量和股四头肌湿重, 计算各组大鼠股四头肌湿重维持率和股四头肌湿重/体质量比值。HE染色观察各组大鼠关节软骨和股四头肌组织病理形态表现, 末端脱氧核苷酸转移酶(TdT)介导的缺口末端标记法(TUNEL)检测各组大鼠关节软骨和股四头肌组织中细胞凋亡指数, 免疫荧光法检测各组大鼠股四头肌组织中白细胞介素6(IL-6)、Janus激酶(JAK)及信号转导与转录激活因子3(STAT3)蛋白表达水平, Western blotting法检测各种大鼠股四头肌组织中IL-6/JAK/STAT3信号通路、肌卫星细胞及凋亡相关蛋白表达水平。**结果:** 与对照组比较, 模型组大鼠患侧后腿围度、股四头肌湿重、湿重维持率和湿重/体质量比值均明显降低($P<0.05$); 与模型组比较, 塞来昔布组和针刺组大鼠患侧后腿围度、股四头肌湿重、湿重维持率和湿重/体质量比值均明显升高($P<0.05$); 与塞来昔布组比较, 针刺组大鼠患侧后腿围度、股四头肌湿重、湿重维持率和湿重/体质量比值均明显升高($P<0.05$)。HE染色观察, 对照组大鼠膝关节软骨保持完整, 软骨细胞聚集且水平排列, 边缘平整, 股四头肌细胞呈长圆柱状, 有序排列, 形态规则; 模型组大鼠膝关节软骨较薄, 边缘粗糙, 软骨层数减少, 排列无序, 股四头肌纤维排列紊乱, 部分肌纤维溶解和肌细胞膜损伤, 并伴有肌纤维碎片和大量炎症渗出液; 塞来昔布组大鼠膝关节软骨形态大体正常, 偶见软骨排列不规律和厚度减少, 偶尔可见散在的坏死软骨细胞, 股四头肌肌纤维和肌膜较为完整, 有新生肌纤维的出现, 部分肌纤维边缘模糊, 伴有少量细胞碎片和轻微炎症浸润; 针刺组大鼠膝关节软骨结构保持完整, 边缘平滑, 偶尔边缘粗糙, 软骨细胞聚集且排列有序。TUNEL法检测, 与对照组比较, 模型组大鼠关节软骨和股四头肌组织中细胞凋亡指数明显升高($P<0.05$); 与模型组比较, 塞来昔布组和针刺组大鼠关节软骨及股四头肌组织中细胞凋亡指数均明显降低($P<0.05$); 与塞来昔布组比较, 针刺组大鼠关节软骨及股四头肌组织中细胞凋亡指数明显降低($P<0.05$)。免疫荧光法检测, 与对照组比较, 模型组大鼠股四头肌组织中IL-6、JAK和STAT3蛋白表达水平均明显降低($P<0.05$); 与模型组比较,

[收稿日期] 2024-12-25 [录用日期] 2025-02-12

[基金项目] 科技部国家重点研发计划项目(2021YFC1712800); 中国博士后科学基金会国家资助博士后研究人员计划项目(GZC20231025); 辽宁省教育厅基本科研项目(JYTQN2023458); 辽宁中医药大学中医脏象理论及应用教育部重点实验室开放基金资助项目(zyzx2410)

[作者简介] 郑曲(1987—), 男, 辽宁省朝阳市人, 讲师, 副主任医师, 医学博士, 主要从事于中医药防治骨性关节炎方面的研究。

[通信作者] 董宝强, 教授, 博士研究生导师(E-mail: peterbaoqiang@163.com);
韩易言, 讲师(E-mail: hyy-zjtn@lnutcm.edu.cn)

©《吉林大学学报(医学版)》编辑部, 开放获取遵循CC BY-NC-ND协议。

© Editorial Board of Journal of Jilin University (Medicine Edition). Open access under CC BY-NC-ND license.

塞来昔布组和针刺组大鼠股四头肌组织中IL-6、JAK及STAT3蛋白表达水平均明显升高 ($P<0.05$); 与塞来昔布组比较, 针刺组大鼠股四头肌组织中IL-6、JAK和STAT3蛋白表达水平均明显升高 ($P<0.05$)。Western blotting法检测, 与对照组比较, 模型组大鼠股四头肌组织IL-6、JAK、STAT3、特异性蛋白配对盒转录因子7 (Pax7)、肌间线蛋白 (Desmin)、肌球蛋白 (Myosin) 和肌细胞生成素 (Myogenin) 蛋白表达水平均明显降低 ($P<0.05$); 与模型组比较, 塞来昔布组和针刺组大鼠股四头肌组织中IL-6、JAK、STAT3、Pax7、Desmin、Myosin和Myogenin蛋白表达水平均明显升高 ($P<0.05$); 与塞来昔布组比较, 针刺组大鼠股四头肌组织中IL-6、JAK、STAT3、Pax7、Desmin、Myosin和Myogenin蛋白表达水平均明显升高 ($P<0.05$)。与对照组比较, 模型组大鼠股四头肌组织中B细胞淋巴瘤2 (Bcl-2), B细胞淋巴瘤xl (Bcl-xl) 和髓系细胞白血病1 (MCL1) 蛋白表达水平均明显降低 ($P<0.05$), Bcl-2相关X蛋白 (Bax) 和半胱氨酸依赖性天冬氨酸特异性蛋白酶3 (Caspase-3) 蛋白表达水平均明显升高 ($P<0.05$); 与模型组比较, 塞来昔布组和针刺组大鼠股四头肌组织中Bcl-2、Bcl-xl和MCL1蛋白表达水平均明显升高 ($P<0.05$), Bax和Caspase-3蛋白表达水平均明显降低 ($P<0.05$); 与塞来昔布组比较, 针刺组大鼠股四头肌组织中Bcl-2、Bcl-xl和MCL1蛋白表达水平均明显升高 ($P<0.05$), Bax和Caspase-3蛋白表达水平均明显降低 ($P<0.05$)。结论: 针刺可促进膝骨关节炎模型大鼠股四头肌卫星细胞分化, 并抑制肌细胞凋亡, 其机制可能与上调股四头肌组织中IL-6、JAK和STAT3蛋白表达有关。

[关键词] 针刺; 白细胞介素6/Janus激酶/信号转导与转录激活因子3信号通路; 肌卫星细胞; 膝骨关节炎模型; 股四头肌

[中图分类号] R684.3 [文献标志码] A

Effect of acupuncture on differentiation and apoptosis of quadriceps muscle satellite cells in knee osteoarthritis model rats and its mechanism

ZHENG Qu^{1,2,3}, DONG Baoqiang^{1,3}, LIN Xingxing^{1,3}, GUAN Xuefeng¹, ZHANG Yu⁴,
WANG Chaojie¹, Han Yiyan¹

(1. College of Acupuncture and massage, Liaoning University of Traditional Chinese Medicine, Shenyang 110847, China; 2. Key Laboratory of Acupuncture and Moxibustion Biology, Education of Liaoning Province, Shenyang 110847, China; 3. Key Laboratory of Acupuncture and Moxibustion Health and Rehabilitation, Shenyang 110847, China; 4. Shenyang Pharmaceutical University, Shenyang 110016, China)

ABSTRACT Objective: To discuss the effect of acupuncture on the differentiation and apoptosis of quadriceps muscle satellite cells in model rats with knee osteoarthritis (KOA), and to clarify its related mechanism. **Methods:** A total of 40 SPF-grade rats were selected and randomly divided into control group, model group, celecoxib group, and acupuncture group, with 10 rats in each group. The rats in control group only underwent joint cavity incision followed by suturing, while the rats in model group, celecoxib group, and acupuncture group were used to replicate the KOA models. The maximum circumference of the femoral segment of the affected limb, rat body mass, and quadriceps wet weight of the rats in various groups were measured; the quadriceps wet weight maintenance rate and quadriceps wet weight/body mass ratio of the rats in various groups were calculated. HE staining was used to observe the pathomorphology of articular cartilage and quadriceps muscle tissue of the rats in various groups; terminal deoxynucleotidyl transferase (TdT)-mediated dUTP nick end labeling (TUNEL) method was used to detect the apoptosis indexes in articular cartilage and quadriceps muscle tissue of the rats in various groups; immunofluorescence method was used to detect the protein expression levels of interleukin-6 (IL-6), Janus kinase (JAK), and

signal transducer and activator of transcription 3 (STAT3) in quadriceps muscle tissue of the rats in various groups; Western blotting method was used to detect the expression levels of IL-6/JAK/STAT3 signaling pathway proteins, and muscle satellite cells, and apoptosis-related proteins in quadriceps muscle tissue of the rats in various groups. **Results:** Compared with control group, the affected hind limb circumference, quadriceps wet weight, wet weight maintenance rate, and wet weight/body mass ratio of the rats in model group were significantly decreased ($P < 0.05$); compared with model group, the affected hind limb circumference, quadriceps wet weight, wet weight maintenance rate, and wet weight/body mass ratio of the rats in celecoxib group and acupuncture group were significantly increased ($P < 0.05$); compared with celecoxib group, the affected hind limb circumference, quadriceps wet weight, wet weight maintenance rate, and wet weight/body mass ratio of the rats in acupuncture group were significantly increased ($P < 0.05$). The HE staining results showed that the knee articular cartilage of the rats in control group remained intact, chondrocytes were aggregated and horizontally arranged with smooth edges, and quadriceps muscle cells were long cylindrical, orderly arranged, and regular in shape; in model group, the knee articular cartilage was thinner with rough edges, reduced number of cartilage layers, and disordered arrangement, and the quadriceps muscle fibers were disorganized, with some muscle fiber dissolution and muscle cell membrane damage, accompanied by muscle fiber fragments and a large amount of inflammatory exudate; in celecoxib group, the morphology of knee articular cartilage was generally normal, occasionally with irregular cartilage arrangement and reduced thickness, sporadically visible necrotic chondrocytes, quadriceps muscle fibers and sarcolemma were relatively intact, new muscle fibers appeared, some muscle fiber edges were blurred, accompanied by a small amount of cell debris and mild inflammatory infiltration; in acupuncture group, the knee articular cartilage structure remained intact with smooth edges, occasionally rough edges, and chondrocytes were aggregated and orderly arranged. The TUNEL assay results showed that compared with control group, the apoptosis indexes in articular cartilage and quadriceps muscle tissue of the rats in model group were significantly increased ($P < 0.05$); compared with model group, the apoptosis indexes in articular cartilage and quadriceps muscle tissue of the rats in celecoxib group and acupuncture group were significantly decreased ($P < 0.05$); compared with celecoxib group, the apoptosis index in articular cartilage and quadriceps muscle tissue of the rats in acupuncture group were significantly decreased ($P < 0.05$). The immunofluorescence assay results showed that compared with control group, the expression levels of IL-6, JAK, and STAT3 proteins in quadriceps muscle tissue of the rats in model group were significantly decreased ($P < 0.05$); compared with model group, the expression levels of IL-6, JAK, and STAT3 proteins in quadriceps muscle tissue of the rats in celecoxib group and acupuncture group were significantly increased ($P < 0.05$); compared with celecoxib group, the expression levels of IL-6, JAK, and STAT3 proteins in quadriceps muscle tissue of the rats in acupuncture group were significantly increased ($P < 0.05$). The Western blotting results showed that compared with control group, the expression levels of IL-6, JAK, STAT3, paired box transcription factor 7 (Pax7), Desmin, Myosin, and Myogenin proteins in quadriceps muscle tissue of the rats in model group were significantly decreased ($P < 0.05$); compared with model group, the expression levels of IL-6, JAK, STAT3, Pax7, Desmin, Myosin, and Myogenin proteins in quadriceps muscle tissue of the rats in celecoxib group and acupuncture group were significantly increased ($P < 0.05$); compared with celecoxib group, the expression levels of IL-6, JAK, STAT3, Pax7, Desmin, Myosin, and Myogenin proteins in quadriceps muscle tissue of the rats in acupuncture group were significantly increased ($P < 0.05$). Compared with control group, the expression levels of B-cell lymphoma 2 (Bcl-2), B-cell lymphoma-x1 (Bcl-x1), and myeloid cell leukemia 1 (MCL1) proteins in quadriceps muscle tissue in model group were significantly decreased ($P < 0.05$), and the expression levels of Bcl-2-associated X protein (Bax) and cysteinyl aspartate specific proteinase-3 (Caspase-3) proteins were significantly increased ($P < 0.05$); compared with model group, the expression levels of

Bcl-2, Bcl-xl, and MCL1 proteins in quadriceps muscle tissue of the rats in celecoxib group and acupuncture group were significantly increased ($P < 0.05$), and the expression levels of Bax and Caspase-3 proteins were significantly decreased ($P < 0.05$); compared with celecoxib group, the expression levels of Bcl-2, Bcl-xl, and MCL1 proteins in quadriceps muscle tissue of the rats in acupuncture group were significantly increased ($P < 0.05$), and the expression levels of Bax and Caspase-3 proteins were significantly decreased ($P < 0.05$). **Conclusion:** Acupuncture can promote the differentiation of quadriceps muscle satellite cells and inhibit muscle cell apoptosis in the model rats with KOA, and the mechanism may be related to the up-regulation of expressions of IL-6, JAK, and STAT3 proteins in the quadriceps muscle tissue.

KEYWORDS Acupuncture; Interleukin-6/Janus kinase/signal transducer and activator of transcription 3 signaling pathway; Muscle satellite cells; Knce osteoarthritis model; Quadriceps muscle

膝骨关节炎(knee osteoarthritis, KOA)是一种以疼痛、僵硬、关节活动减少和肌肉无力为症状和体征的慢性关节疾病,其主要影响膝关节软骨、软骨下骨、滑膜和关节相关肌肉肌腱的功能,是全球老年人致残的主要原因之一^[1]。预计至2050年, KOA病例将增加74.9%^[2]。《2024中国膝骨关节炎临床药物治疗专家共识》^[3]中指出:我国男性KOA患病率为11%,女性患病率为19%,且随着人口老龄化和肥胖问题的增加,其发病率呈显著上升趋势,成为影响我国老年社会参与的最主要原因之一。人体为直立行走的生物体,膝关节周围肌肉对于维持人的体力线稳定至关重要,其不仅提供动力支持,还通过与关节囊相交织增加膝关节的动态稳定性。《膝骨关节炎中西医结合诊疗指南(2023版)》^[4]中指出:KOA患者伸肌群存在明显的肌肉萎缩,表明KOA的发病与关节周围的肌肉病变存在相关性。本课题组前期研究^[5]证实:KOA患者膝关节周围存在肌肉力量不平衡,当一侧肌肉紧张引起肌力下降,另外一侧肌力正常时,人体力线会偏向正常一侧,因此当伸肌肌群(股四头肌为主)萎缩后,人体力线会偏向屈肌群,即人体的后侧线,而肌肉持续紧张后,会出现肌纤维凋亡的情况^[6]。肌纤维的再生由肌卫星细胞分化而来^[7]。因此,针刺是否能够通过改善肌卫星细胞的分化而增加肌纤维再生,增强患侧肌力进而对KOA起保护作用尚未完全阐明。本研究以白细胞介素6(interleukin-6, IL-6)/Janus激酶(Janus kinase, JAK)/信号转导与转录激活因子3(signal transducer and activator of transcription 3, STAT3)信号通路为切入点,观察针刺治疗KOA的临床疗效,为针刺治疗KOA提供理论依据。

1 材料与方法

1.1 实验动物、针具、药物、主要试剂和仪器 选取40只SPF级Wistar大鼠,购自辽宁长生生物技术股份有限公司,实验动物生产许可证号:SCXK(辽)2019-0001。实验动物饲养于辽宁中医药大学动物实验中心,饲养条件安静通风,湿度50%,温度恒温26℃,大鼠自由饮水,饲用标准饲料,定期更换饲料,并消毒。本研究严格遵循《实验动物管理条例》进行相关操作,且通过辽宁中医药大学伦理委员会批准,伦理审批号:21000042023118。华佗牌针灸针购自苏州医疗用品有限公司。塞来昔布胶囊购自美国辉瑞制药有限公司,国药准字HJ20140106。 β -肌动蛋白(β -actin)和辣根过氧化物酶(horseradish peroxidase, HRP)均购自武汉三鹰生物技术有限公司,末端脱氧核苷酸转移酶(terminal deoxynucleotidyl transferase, TdT)介导的缺口末端标记法(TdT-mediated dUTP nick-end labeling, TUNEL)染色试剂盒购自上海弗元生物科技有限公司,IL-6、JAK抗体、STAT3、肌卫星细胞特异性蛋白配对盒转录因子7(paired box transcription factor 7, Pax7)抗体、重组肌间线蛋白(Desmin)抗体、抗肌球蛋白(Myosin)抗体和抗肌细胞生成素(Myogenin)抗体均购自艾博抗(上海)贸易有限公司, B细胞淋巴瘤xl(B-cell lymphoma-xl, Bcl-xl)抗体、B细胞淋巴瘤2(B-cell lymphoma-2, Bcl-2)抗体、Bcl-2相关X蛋白(Bcl-2-associated X protein, Bax)抗体、髓系细胞白血病1(myeloid cell leukemia 1, MCL1)抗体和半胱氨酸依赖性天冬氨酸特异性蛋白酶3(cysteine-dependent aspartate-specific protease-3, Caspase-3)抗体均购自武汉三鹰生物技术有限公司。BX53型荧光显微镜购自日本OLYMPUS公

司, MB-530型多功能酶标分析仪购自深圳市汇松科技发展有限公司, DM500光学显微镜购自德国Leica公司, EPS-600电泳仪、VE-180电泳槽和VE-186转膜仪均购自上海天能生命科学有限公司。

1.2 大鼠KOA模型制备、动物分组和处理 所有大鼠适应性饲养1周后, 随机分为对照组、模型组、塞来昔布组和针刺组, 每组各10只。所有大鼠禁食不禁水24 h后, 20% 乌来糖(乌拉坦和氨基甲酸乙酯)麻醉, 对照组大鼠仅切开关节腔后缝合, 模型组、塞来昔布组和针刺组大鼠采用改良Hulth方法^[8]构建KOA模型。模型复制成功后, 采用HE染色法观察大鼠膝骨关节软骨形态表现, 验证大鼠造模情况。模型复制成功后, 对照组和模型组大鼠给予生理盐水灌胃, 塞来昔布组大鼠给予浓度 $1.8\text{ g}\cdot\text{L}^{-1}$ 塞来昔布溶液灌胃, 针刺组大鼠选取髌下、鹤顶次和血海次进行针刺^[9]。穴位定位: 髌下位于膝部, 髌韧带下缘; 鹤顶次位于膝部, 髌骨上缘; 血海次位于股内侧部, 膝内缘直上与缝匠肌交界处, 动物解剖结构与人类相同。毫针直刺至骨面, 反复提插约10次刺激肌肉或韧带与骨面连接处, 留针20 min, 各组大鼠每日干预1次, 连续干预14 d。在干预过程中, 大鼠仍进行被动运动。

1.3 样本采集和处理 各组大鼠末次干预后, 12 h禁食水, 乌来糖麻醉后, 固定于操作台上, 测量大鼠患肢股骨段最大周长和大鼠体质量。完整取下大鼠双下肢的股四头肌, 测量其湿重, 计算其股四头肌湿重维持率和股四头肌的湿重/体质量比值。股四头肌湿重维持率=患侧肌肉湿重(mg)/健侧肌肉湿重(mg) $\times 100\%$ 。湿重/体质量比值=患侧肌肉湿重(mg)/总体质量(mg)。

1.4 HE染色观察各组大鼠关节软骨和股四头肌组织病理形态表现 每组取5只大鼠, 将大鼠患侧股四头肌和关节软骨置于多聚甲醛中固定72 h, 关节软骨需要做脱钙处理4周, 石蜡包埋切片, 经苏木素染、氨水返蓝和伊红染色, 乙醇梯度脱水, 最后二甲苯透明, 中性树胶封片。使用400倍光学显微镜观察各组大鼠关节软骨和股四头肌组织病理形态表现。

1.5 TUNEL法检测各组大鼠软骨细胞和股四头肌组织中细胞凋亡指数 取大鼠股四头肌切片和脱钙后的关节软骨切片, 清洗封闭, 滴加TdT孵育缓冲液50 μL , 孵育1 h, 磷酸盐缓冲液(phosphate buffered saline, PBS)冲洗切片, 滴加

一抗4 $^{\circ}\text{C}$ 过夜。后滴加荧光二抗50 μL , 孵育1.5 h, 用4', 6-二脒基-2-苯基吲哚(4', 6-diamidino-2-phenylindole, DAPI)染细胞核呈蓝色, 孵育, 封片。荧光显微镜下观察, 并拍照, 每个样本选取3个视野, 采用Image J软件计数TUNEL阳性细胞数和总细胞数(DAPI阳性), 计算TUNEL阳性细胞比值。TUNEL阳性细胞比值=TUNEL阳性细胞数/DAPI阳性细胞数, 以TUNEL阳性细胞比值代表细胞凋亡指数。

1.6 免疫荧光法检测各组大鼠股四头肌组织中IL-6、JAK和STAT3蛋白表达水平 各组大鼠股四头肌组织的石蜡切片进行抗原修复, 修复后滴加一抗孵育(1:100), 4 $^{\circ}\text{C}$ 过夜, PBS缓冲液清洗后滴加荧光二抗(1:200)和DAPI, 孵育1 h。滴加荧光淬灭剂, 封片。荧光显微镜下观察, 并拍照, 每个样本选取3个视野。采用Image J软件分析各组大鼠股四头肌组织中相关蛋白荧光强度, 以荧光强度代表目的蛋白表达水平。

1.7 Western blotting法检测各组大鼠股四头肌组织中IL-6/JAK/STAT3信号通路、肌卫星细胞及凋亡相关蛋白表达水平 提取大鼠股四头肌组织中的总蛋白, EPS-600电泳仪进行电泳, 分离目标蛋白。转膜、封闭, 清洗后, 孵育相关一抗(1:2500), 4 $^{\circ}\text{C}$ 孵育12 h。第2天已孵育一抗的PVDF孵育于二抗(1:2000)中2 h, TBS溶液洗涤后, 采用天能5200曝光机进行拍摄, Image J软件分析IL-6、JAK、STAT3、Pax7、Desmin、Myosin、Myogenin、Bcl-2、Bcl-xl、Bax、MCL1和Caspase-3蛋白条带灰度值, 以 β -actin为内参, 计算目的蛋白表达水平。目的蛋白表达水平=目的蛋白条带灰度值/内参蛋白条带灰度值。每种蛋白检测3次, 取平均值。

1.8 统计学分析 采用SPSS 25.0软件进行统计学分析。各组大鼠患侧后腿围度、湿重、湿重维持率、湿重/体质量比值、股四头肌肌细胞凋亡率、股四头肌组织中IL-6/JAK/STAT3信号通路和肌卫星细胞及凋亡相关蛋白表达水平符合正态分布, 以 $\bar{x}\pm s$ 表示, 多组间样本均数比较采用单因素方差分析, 组间样本均数两两比较采用独立样本 t 检验。以 $P<0.05$ 为差异有统计学意义。

2 结果

2.1 各组患侧后腿的周长、股四头肌湿重、湿重维持率和股四头肌湿重/体质量比值 与对照组比较, 模型组大鼠患侧后腿围度、股四头肌湿重、湿重维

持率和湿重/体质量比值均明显降低 ($P<0.05$)。与模型组比较,塞来昔布组和针刺组大鼠患侧后腿围度、股四头肌湿重、湿重维持率及湿重/体质量比值均

明显升高 ($P<0.05$);与塞来昔布组比较,针刺组大鼠患侧后腿围度、股四头肌湿重、湿重维持率和湿重/体质量比值均明显升高 ($P<0.05$)。见表1。

表1 各组大鼠患侧后腿围度、股四头肌湿重、湿重维持率和湿重/体质量比值

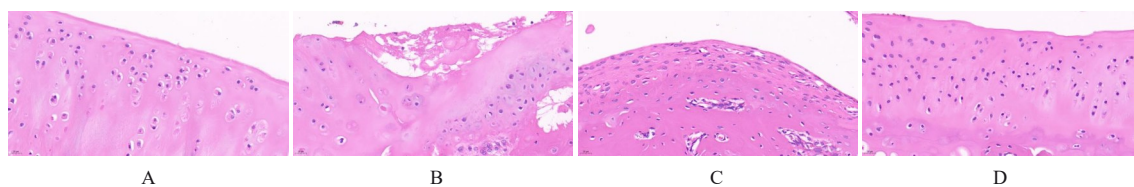
Tab. 1 Circumferences of affected hind leg, wet weight of quadriceps femoris muscle, wet weight maintenance rates, and wet weight/body mass ratios of rats in various groups ($\bar{x}\pm s, n=9$)

Group	Circumference(<i>l</i> /mm)	Wet weight (<i>m</i> /g)	Wet weight maintenance rate(η /%)	Ratio of wet weight/body mass
Control	157.44 \pm 11.88	5.17 \pm 0.84	95.78 \pm 2.17	4.78 \pm 0.67
Model	99.33 \pm 11.16*	3.00 \pm 0.50*	82.67 \pm 5.20*	2.33 \pm 0.50*
Celecoxib	105.56 \pm 13.51 Δ	3.78 \pm 0.67 Δ	86.67 \pm 3.67 Δ	3.00 \pm 0.87 Δ
Acupuncture	134.22 \pm 16.52 Δ [#]	4.56 \pm 0.53 Δ [#]	94.33 \pm 2.69 Δ [#]	4.56 \pm 0.73 Δ [#]

* $P<0.05$ vs control group; $\Delta P<0.05$ vs model group; [#] $P<0.05$ vs celecoxib group.

2.2 各组大鼠膝关节软骨病理形态表现 对照组大鼠膝关节软骨保持完整,软骨细胞聚集且水平排列,边缘平整。模型组大鼠膝关节软骨较薄,边缘粗糙,软骨层数减少,排列无序,可见因脱水导致的软骨细胞萎缩坏死,各层难以区分。塞来昔

布组大鼠膝关节软骨形态大体正常,偶见软骨排列不规律和厚度减少,偶尔可见散在的坏死软骨细胞。针刺组大鼠膝关节软骨结构保持完整,边缘平滑,偶尔边缘粗糙,软骨细胞聚集且排列有序。见图1。



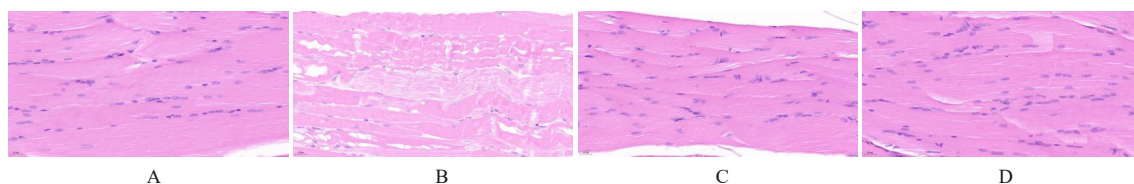
A:Control group; B:Model group; C:Celecoxib group; D:Acupuncture group.

图1 各组大鼠膝关节软骨病理形态表现(HE, $\times 400$)

Fig. 1 Pathomorphology of articular cartilage of rats in various groups (HE, $\times 400$)

2.3 各组大鼠股四头肌组织病理形态表现 对照组大鼠股四头肌组织中细胞呈长圆柱状,有序排列,形态规则,可见细胞核蓝染位于肌纤维表面,较为完整。模型组大鼠股四头肌纤维排列紊乱,可见部分肌纤维溶解,可见到肌细胞膜损伤,表面不平,较为

分散,间隙明显,并伴有肌纤维碎片和大量炎症渗出液,淋巴细胞数量增加。塞来昔布组和针刺组大鼠股四头肌肌纤维大多保持了完整的长圆柱形,肌膜较为完整,有新生肌纤维的出现,部分肌纤维边缘模糊,伴有少量细胞碎片和轻微炎症浸润。见图2。



A:Control group; B:Model group; C:Celecoxib group; D:Acupuncture group.

图2 各组大鼠股四头肌组织病理形态表现(HE, $\times 400$)

Fig. 2 Pathomorphology of quadriceps muscle tissue of rats in various groups (HE, $\times 400$)

2.4 各组大鼠关节软骨和股四头肌组织中细胞凋亡指数 与对照组比较,模型组大鼠关节软骨和

股四头肌组织中细胞凋亡指数明显升高 ($P<0.05$)。与模型组比较,塞来昔布组和针刺组大鼠关节软骨及

股四头肌组织中细胞凋亡指数均明显降低 ($P < 0.05$)。与塞来昔布组比较, 针刺组大鼠关节软骨及

股四头肌组织中细胞凋亡指数明显降低 ($P < 0.05$)。见图 3、图 4 和表 2。

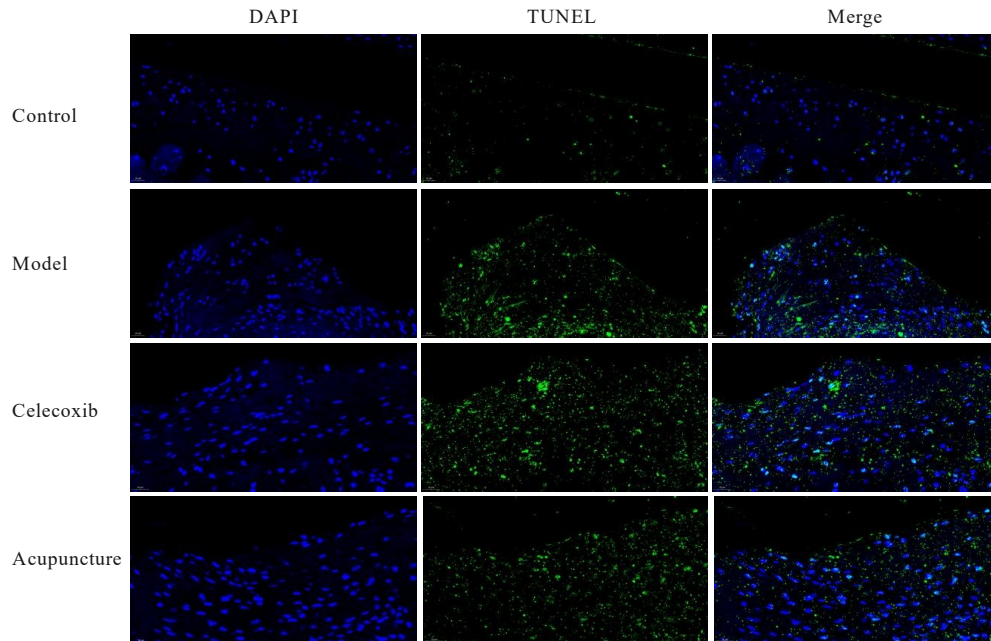


图 3 TUNEL 法检测各组大鼠关节软骨细胞凋亡情况(×400)

Fig. 3 Apoptosis of articular cartilage cells of rats in various groups detected by TUNEL method (×400)

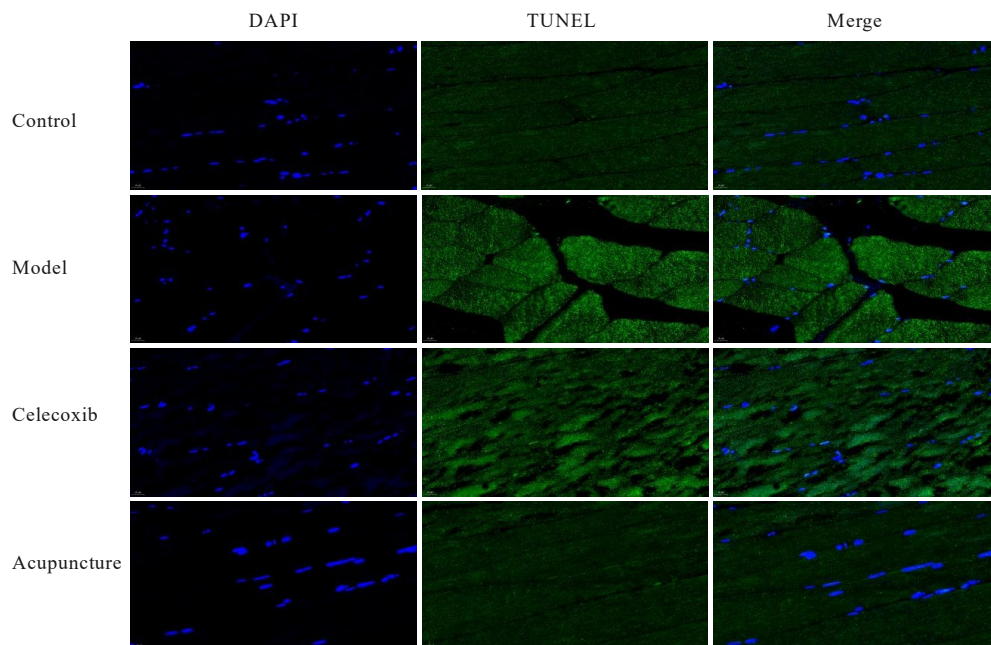


图 4 TUNEL 法检测各组大鼠股四头肌组织中细胞凋亡情况(×400)

Fig. 4 Apoptosis in quadriceps muscle tissue of rats in various groups detected by TUNEL method (×400)

2.5 各组大鼠股四头肌组织中 IL-6、JAK 和 STAT3 蛋白表达水平 与对照组比较, 模型组大鼠股四头肌组织中 IL-6、JAK 和 STAT3 蛋白表达水平均明显降低 ($P < 0.05$)。与模型组比较, 塞

来昔布组和针刺组大鼠股四头肌组织中 IL-6、JAK 及 STAT3 蛋白表达水平均明显升高 ($P < 0.05$)。与塞来昔布组比较, 针刺组大鼠股四头肌组织中 IL-6、JAK 和 STAT3 蛋白表达水平均明显升高 ($P <$

表2 各组大鼠关节软骨和股四头肌组织中细胞凋亡指数
Tab. 2 Comparison of apoptosis index of articular cartilage and quadriceps femoris muscle tissue of rats in various groups
($n=9, \bar{x} \pm s$)

Group	Apoptosis index	
	Articular cartilage	Quadriceps femoris muscle tissue
Control	0.62±0.10	0.78±0.19
Model	1.52±0.29*	2.42±0.37*
Celecoxib	1.34±0.19 [△]	1.56±0.24 [△]
Acupuncture	1.03±0.21 ^{△#}	0.91±0.18 ^{△#}

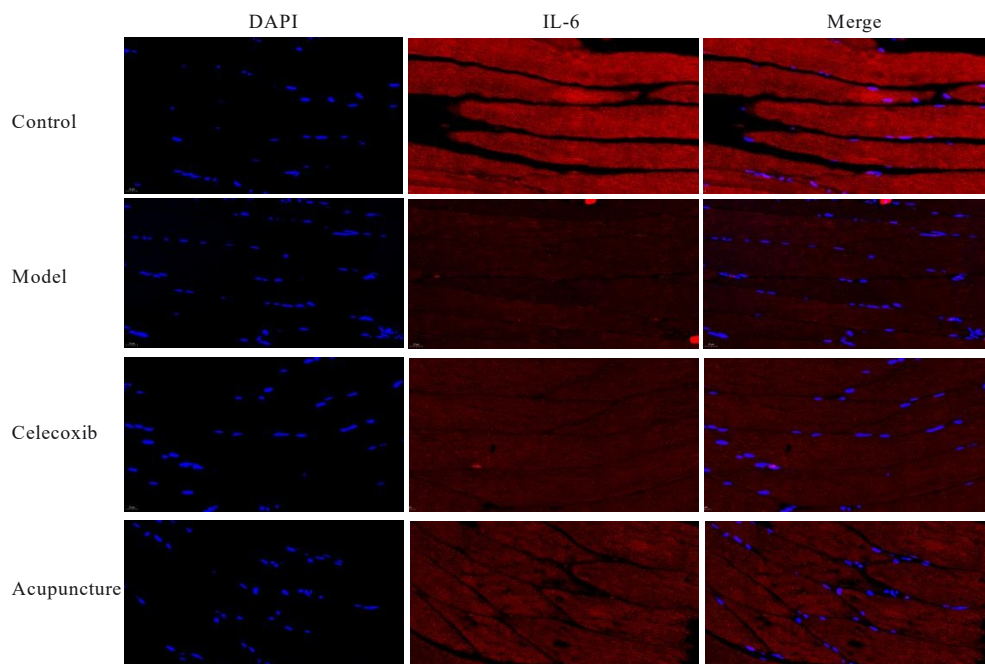
* $P<0.05$ vs control group; [△] $P<0.05$ vs model group; [#] $P<0.05$ vs celecoxib group.

0.05)。见图5~7和表3。

2.6 各组大鼠股四头肌组织中IL-6、JAK和STAT3蛋白表达水平 与对照组比较,模型组大鼠股四头肌组织中IL-6、JAK和STAT3蛋白表达水平均明显降低($P<0.05$)。与模型组比较,塞来昔布组和针刺组大鼠股四头肌组织中IL-6、JAK及STAT3蛋白表达水平均明显升高($P<0.05$)。与塞来昔布组比较,针刺组大鼠股四头肌组织中IL-6、JAK和STAT3蛋白表达水平均明显升高($P<0.05$)。见图8和表4。

2.7 各组大鼠股四头肌组织中卫星细胞特异性蛋白表达水平 与对照组比较,模型组大鼠股四头肌组织中Pax7、Desmin、Myosin和Myogenin蛋白表达水平均明显降低($P<0.05$)。与模型组比较,塞来昔布组和针刺组大鼠股四头肌组织中Pax7、Desmin、Myosin和Myogenin蛋白表达水平均明显升高($P<0.05$)。与塞来昔布组比较,针刺组大鼠股四头肌组织中Pax7、Desmin、Myosin和Myogenin蛋白表达水平均明显升高($P<0.05$)。见图9和表5。

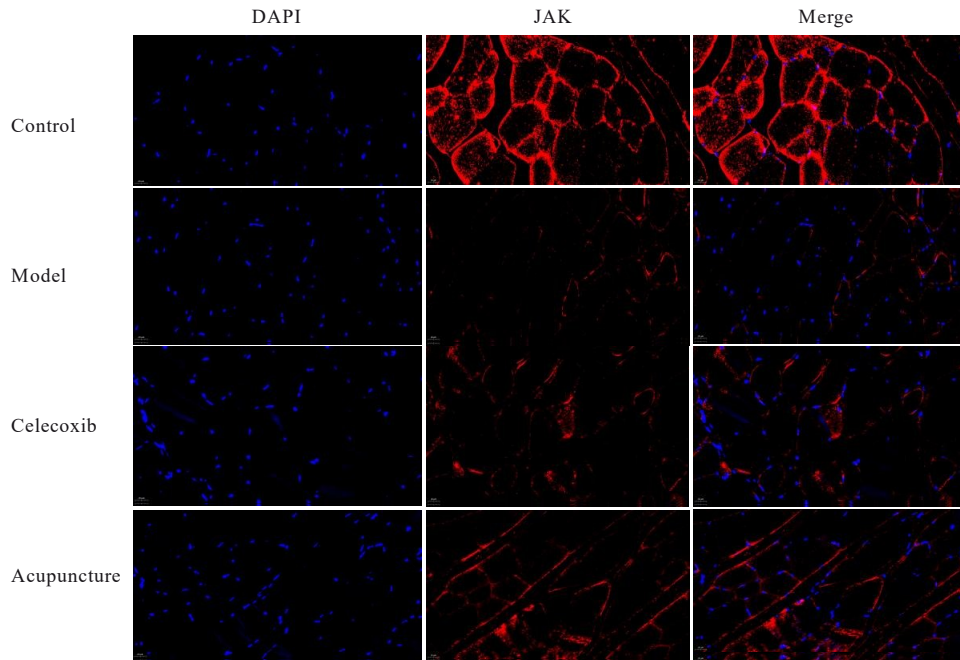
2.8 各组大鼠股四头肌组织中凋亡相关蛋白Bcl-2、Bcl-x1、Bax、MCL1和Caspase-3蛋白表达水平 与对照组比较,模型组大鼠股四头肌组织中Bcl-2、Bcl-x1和MCL1蛋白表达水平均明显降低($P<0.05$),Bax和Caspase-3蛋白表达水平均明显升高($P<0.05$)。与模型组比较,塞来昔布组和针刺组大鼠股四头肌组织中Bcl-2、Bcl-x1和MCL1蛋白表达水平均明显升高($P<0.05$),Bax和Caspase-3蛋白表达水平均明显降低($P<0.05$)。与塞来昔布组比较,针刺组大鼠股四头肌组织中Bcl-2、Bcl-x1和MCL1蛋白表达水平均明显升高($P<0.05$),Bax和Caspase-3蛋白表达水平均明显降低($P<0.05$)。见图10和表6。



Blue represented nuclear staining, and red represented fluorescence expression of IL-6 protein.

图5 免疫荧光法检测各组大鼠股四头肌组织中IL-6蛋白表达情况(×400)

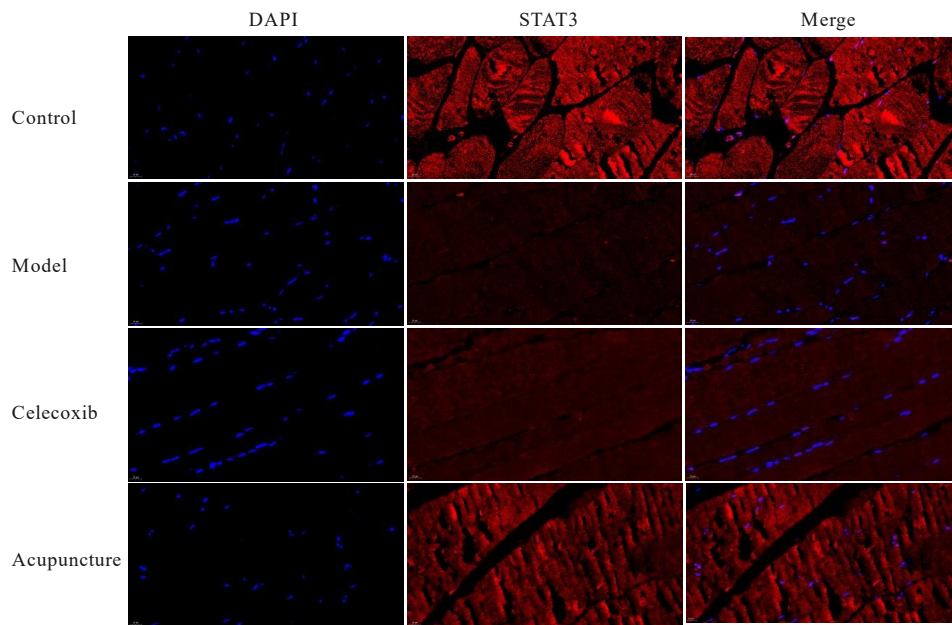
Fig. 5 Expressions of IL-6 protein in quadriceps muscle tissue of rats in various groups detected by immunofluorescence assay (×400)



Blue represented nuclear staining, and red represented fluorescence expression of JAK protein.

图 6 免疫荧光法检测各组大鼠股四头肌组织中 JAK 蛋白表达情况(×400)

Fig. 6 Expressions of JAK protein in quadriceps muscle tissue of rats in various groups detected by immunofluorescence assay (×400)



Blue represented nuclear staining, and red represented fluorescence expression of STAT3 protein.

图 7 免疫荧光法检测各组大鼠股四头肌组织中 STAT3 蛋白表达情况(×400)

Fig. 7 Expressions of STAT3 protein in quadriceps muscle tissue of rats in various groups detected by immunofluorescence assay (×400)

3 讨 论

KOA 是一种主要影响中老年人群的常见疾病, 其病理改变涉及软骨、软骨下骨和滑膜, 但随着对

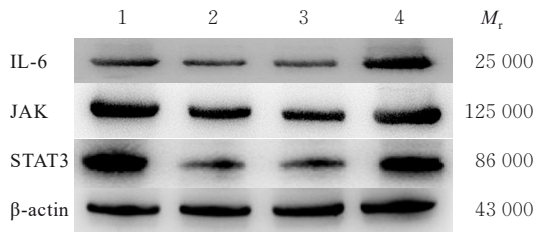
该病的深入研究发现: 膝关节周围的肌肉和韧带功能障碍也是造成膝关节炎的原因之一^[10]。研究^[11]显示: KOA 与关节周围肌力下降高度有关, 且以伸肌肌力下降为主, 膝关节主要的伸肌即为股

表3 各组大鼠股四头肌组织中IL-6、JAK和STAT3蛋白表达水平

Tab. 3 Expression levels of IL-6, JAK, and STAT3 proteins in quadriceps muscle tissue of rats in various groups (n=9, $\bar{x} \pm s$)

Group	IL-6	JAK	STAT3
Control	12.04±2.12	10.02±1.73	9.83±1.45
Model	1.02±0.21*	1.45±0.31*	2.72±0.36*
Celecoxib	5.13±1.25 [△]	6.23±1.12 [△]	5.24±1.19 [△]
Acupuncture	9.14±1.32 ^{△#}	8.07±1.53 ^{△#}	9.02±0.54 ^{△#}

*P<0.05 vs control group; [△]P<0.05 vs model group; [#]P<0.05 vs celecoxib group.



Lane 1: Control group; Lane 2: Model group; Lane 3: Celecoxib group; Lane 4: Acupuncture group.

图8 Western blotting法检测各组大鼠股四头肌组织中IL-6、JAK和STAT3蛋白表达电泳图

Fig. 8 Electrophoregram of expressions of IL-6, JAK, and STAT3 proteins in quadriceps muscle tissue of rats in various groups detected by Western blotting method

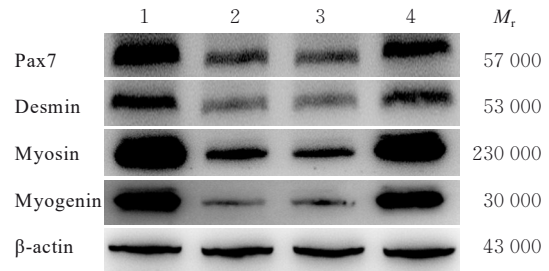
表4 各组大鼠股四头肌组织中IL-6、JAK和STAT3蛋白表达水平

Tab. 4 Expression levels of IL-6, JAK, and STAT3 proteins in quadriceps muscle tissue of rats in various groups (n=9, $\bar{x} \pm s$)

Group	IL-6	JAK	STAT3
Control	0.73±0.13	0.83±0.13	0.98±0.16
Model	0.12±0.08*	0.44±0.10*	0.21±0.09*
Celecoxib	0.52±0.10 [△]	0.53±0.12 [△]	0.76±0.10 [△]
Acupuncture	0.80±0.15 ^{△#}	0.76±0.17 ^{△#}	0.81±0.12 ^{△#}

*P<0.05 vs control group; [△]P<0.05 vs model group; [#]P<0.05 vs celecoxib group.

四头肌, 因此股四头肌的肌力下降是KOA发病的重要原因之一。经筋是经络系统中的一部分, 其主要作用是约束骨骼, 利于关节屈伸活动^[12]。《黄帝内经》:“骨正筋柔, 气血以流”, 若“筋不柔”则“骨不正”。本课题组多年以来致力于经筋医学的研究, 通过针刺相应的经筋病灶点可以恢复肌肉张



Lane 1: Control group; Lane 2: Model group; Lane 3: Celecoxib group; Lane 4: Acupuncture group.

图9 各组大鼠股四头肌组织中肌卫星细胞特异性蛋白表达电泳图

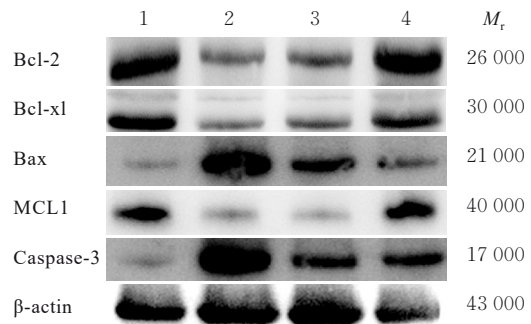
Fig. 9 Electrophoregram of expressions of satellite cell specific proteins in quadriceps muscle tissue of rats in various groups

表5 各组大鼠股四头肌组织中肌卫星细胞特异性蛋白表达水平

Tab. 5 Expression levels of muscle satellite cell specific proteins in quadriceps muscle tissue of rats in various groups (n=9, $\bar{x} \pm s$)

Group	Pax7	Desmin	Myosin	Myogenin
Control	0.87±0.13	0.72±0.13	0.90±0.07	0.81±0.12
Model	0.15±0.03*	0.10±0.05*	0.14±0.04*	0.24±0.08*
Celecoxib	0.67±0.10 [△]	0.51±0.12 [△]	0.49±0.15 [△]	0.62±0.17 [△]
Acupuncture	0.72±0.16 ^{△#}	0.70±0.13 ^{△#}	0.74±0.12 ^{△#}	0.83±0.21 ^{△#}

*P<0.05 vs control group; [△]P<0.05 vs model group; [#]P<0.05 vs celecoxib group.



Lane 1: Control group; Lane 2: Model group; Lane 3: Celecoxib group; Lane 4: Acupuncture group.

图10 各组大鼠股四头肌组织中Bcl-2、Bcl-xl、Bax、MCL1和Caspase-3蛋白表达电泳图

Fig. 10 Electrophoregram of expressions of Bcl-2, Bcl-xl, Bax, MCL1, and Caspase-3 proteins in quadriceps muscle tissue of rats in various groups

力, 纠正关节力线, 在长期的运动中达到“骨正筋柔”的状态, 减少软骨的磨损^[13-14]。研究^[15-16]显示:

表6 各组大鼠股四头肌组织中凋亡相关蛋白表达水平

Tab. 6 Expression levels of apoptosis-related proteins in quadriceps muscle tissue of rats in various groups ($n=9, \bar{x} \pm s$)

Group	Bcl-2	Bcl-xl	Bax	MCL1	Caspase-3
Control	0.91±0.13	0.94±0.14	0.13±0.02	0.70±0.13	0.09±0.01
Model	0.13±0.02*	0.10±0.02*	0.92±0.10*	0.15±0.02*	0.93±0.12*
Celecoxib	0.21±0.04 [△]	0.31±0.07 [△]	0.48±0.12 [△]	0.23±0.03 [△]	0.62±0.13 [△]
Acupuncture	0.83±0.12 ^{△#}	0.78±0.12 ^{△#}	0.19±0.04 ^{△#}	0.73±0.12 ^{△#}	0.36±0.06 ^{△#}

* $P<0.05$ vs control group; [△] $P<0.05$ vs model group; [#] $P<0.05$ vs celecoxib group.

KOA模型大鼠股四头肌出现凋亡、焦亡增加,进而导致股四头肌萎缩,股四头肌萎缩后,肌力更加下降,导致力线更加偏移,加重关节表面软骨的磨损,加重KOA的症状,形成了恶性循环,因此加速股四头肌肌肉的恢复是治疗本病的一个突破点。

肌卫星细胞是骨骼肌特有的干细胞,位于肌纤维的基质膜与基底膜之间,对肌肉的再生及增殖至关重要,在动物成年之后便具有增殖和分化潜能,作为骨骼肌的成体干细胞,有助于肌肉的生长、修复和再生^[17]。当细胞被肌源性激活时,卫星细胞会增殖并分化成新的肌纤维。肌卫星细胞中存在Pax7、Desmin、Myosin和Myogenin蛋白等特异性蛋白^[18-20]。其中,Pax7是肌卫星细胞的一个特异性标志物,其在肌卫星细胞的自我更新和分化中扮演重要角色;Desmin也称结蛋白,是一种中间丝蛋白,是肌卫星细胞的一个早期标志物,其在肌卫星细胞的分化过程中起重要作用;Myosin是肌肉收缩过程中的关键蛋白,其表达增加通常标志着肌卫星细胞分化为肌纤维的后期阶段;Myogenin是肌卫星细胞分化过程中的一个晚期标志物,其在肌卫星细胞的终末分化和肌纤维形成中起重要作用。JAK/STAT3信号通路是一种进化上保守的信号通路,由细胞因子刺激激活,使细胞外信号通过细胞膜传递到细胞核,引起DNA转录的改变,在几个关键的生理过程中发挥作用^[21-23]。在骨骼肌再生过程中,肌卫星细胞的激活、增殖和分化是关键步骤。IL-6可通过JAK2/STAT3信号通路调节肌卫星细胞的增殖和分化。然而,持续高水平的IL-6信号可能会对肌卫星细胞产生负面影响。例如,在老年小鼠中,IL-6信号的持续升高会导致肌肉干细胞衰竭及肌肉萎缩。此外,JAK2/STAT3信号通路的异常激活也可能抑制肌卫星细胞的增殖,进而影响骨骼肌的再生能力。而在骨骼肌细胞凋亡方面,JAK2/STAT3信号通路的激活与细胞凋亡密切相关。研究^[24]发现:赖氨酸缺乏可通过激活

JAK2/STAT3信号通路诱导猪骨骼肌卫星细胞凋亡,表明JAK2/STAT3信号通路的过度激活可能通过上调凋亡相关蛋白(如Caspase-3和Bax)的表达,促进肌卫星细胞的凋亡。本研究结果显示:KOA模型大鼠股四头肌组织中IL-6、JAK和STAT3蛋白呈低表达状态,通过塞来昔布和针刺膝下、鹤顶穴及血海穴干预,可以明显升高股四头肌组织中IL-6、JAK和STAT3蛋白表达水平,且针刺组优于塞来昔布组。针刺激活IL-6、JAK和STAT3蛋白后,IL-6可以通过与细胞表面的受体结合,激活受体相关的JAK2。JAK2进一步磷酸化受体,为STAT3提供结合位点,磷酸化的STAT3形成二聚体,并转移到细胞核内。在细胞核内,STAT3结合到特定基因的启动子区域,调控基因表达,STAT3激活后,可以促进细胞周期蛋白D1等基因的表达,这些基因对于细胞从细胞周期G₁期进入S期至关重要,从而促进肌卫星细胞的增殖和分化,同时通过调控一系列与肌肉生成相关的基因,JAK/STAT3信号通路能够促进肌卫星细胞分化为成熟的肌管,增强肌肉功能恢复。本研究结果显示:与模型组比较,针刺组大鼠股四头肌组织中Bcl-2、Bcl-xl和MCL1蛋白表达水平较高,Bax和Caspase-3蛋白表达水平较低,因针刺激活STAT3在细胞核内还可以激活抗凋亡基因的表达,如Bcl-2。Bcl-2蛋白能够抑制细胞凋亡,通过阻断细胞凋亡途径中的关键因子(如Caspase-3和Bax),减少细胞凋亡。同时JAK/STAT3通路的激活可以抑制凋亡相关信号通路,如抑制Caspase-3和Bax的表达。相关凋亡因子的减少有助于维持肌卫星细胞的存活,减少因凋亡导致的肌肉细胞丢失。

综上所述,针刺可促进KOA模型大鼠股四头肌卫星细胞分化,并抑制肌细胞凋亡,其机制可能与上调股四头肌组织中IL-6、JAK和STAT3蛋白表达有关。

利益冲突声明:

所有作者声明不存在利益冲突。

作者贡献声明:

郑曲参与实验操作和论文撰写,董宝强参与论文总体设计和审阅,林星星和张宇参与实验操作,关雪峰参与实验设计和基金支持,王超杰参与数据统计学分析,韩易言参与论文审阅。

[参考文献]

- [1] ABRAMOFF B, CALDERA F E. Osteoarthritis [J]. *Med Clin N Am*, 2020, 104(2): 293-311.
- [2] 谢文慧,张卓莉.难治性类风湿关节炎的治疗策略[J].*中国实用内科杂志*, 2024, 44(12): 1006-1010.
- [3] 中国医师协会风湿免疫科医师分会骨关节炎学组.中国膝关节炎临床药物治疗专家共识(2023)[J].*中华内科杂志*, 2024, 63(6): 560-578.
- [4] 中华中医药学会.膝关节炎中西医结合诊疗指南(2023年版)[J].*中医正骨*, 2023, 35(6): 1-10.
- [5] 郑曲,林星星,张宇,等.基于Piezo1/YAP/Caspase3轴探讨针刺保护膝骨性关节炎模型大鼠股四头肌细胞的机制研究[J].*世界科学技术-中医药现代化*, 2025, 27(8): 2274-2283.
- [6] YANG X F, XUE P P, CHEN H R, et al. Denervation drives skeletal muscle atrophy and induces mitochondrial dysfunction, mitophagy and apoptosis *via* miR-142a-5p/MFN1 axis[J]. *Theranostics*, 2020, 10(3): 1415-1432.
- [7] 李嫣晓,陈红霞,程梦蝶,等.铁死亡与心肌纤维化相关信号通路的研究进展[J].*郑州大学学报(医学版)*, 2024, 59(2): 195-201.
- [8] LIU X X, LI X H, ZHOU J T. Experimental study on replicating knee osteoarthritis by modified Hulth's modeling method[J]. *Zhongguo Zhong Xi Yi Jie He Za Zhi*, 2005, 25(12): 1104-1108.
- [9] 薛立功.经筋理论研究对经络学说形成的启迪意义[A].//中国针灸学会经筋诊治专业委员会成立大会暨首届中华经筋医学论坛论文集[C]. 2009: 1-7.
- [10] APURBA G, SUDIP B. Biomonitoring the skeletal muscle metabolic dysfunction in knee osteoarthritis in older adults: Is Jumpstart Nutrition[®] Supplementation effective[J]. *Caspian J Intern Med*, 2023, 14(4): 590-606.
- [11] 中医康复临床实践指南·膝关节炎制定工作组,王尚全,朱立国,等.中医康复临床实践指南·膝关节炎[J].*康复学报*, 2020, 30(3): 177-182.
- [12] 林星星,董宝强,王树东,等.基于筋膜的经筋基础研究:述评与展望[J].*中国针灸*, 2023, 43(11): 1338-1342.
- [13] 罗序国,熊明洁,江睿.基于“宗筋主束骨而利机关”理论的中医手法治疗膝骨关节炎的临床观察[J].*中国医学创新*, 2022, 19(21): 86-90.
- [14] 贺文华,董晓慧,汤臣建,等.“宗筋主束骨而利机关”理论在经筋病中的临床应用概况[J].*湖南中医杂志*, 2019, 35(5): 155-157.
- [15] COLETTI C, ACOSTA G F, KESLACY S, et al. Exercise-mediated reinnervation of skeletal muscle in elderly people: an update[J]. *Eur J Transl Myol*, 2022, 32(1): 10416.
- [16] ZHENG D D, LIU J, PIAO H L, et al. ROS-triggered endothelial cell death mechanisms: Focus on pyroptosis, parthanatos, and ferroptosis[J]. *Front Immunol*, 2022, 13: 1039241.
- [17] 黄吴心蕊,田静,贺洁宇.原发性干燥综合征合并骨质疏松的危险因素[J].*中南大学学报(医学版)*, 2024, 49(2): 312-318.
- [18] SOUSA-VICTOR P, GARCÍA-PRAT L, MUÑOZ-CÁNOVES P. Control of satellite cell function in muscle regeneration and its disruption in ageing [J]. *Nat Rev Mol Cell Biol*, 2022, 23(3): 204-226.
- [19] KUANG S H, KURODA K, LE GRAND F, et al. Asymmetric self-renewal and commitment of satellite stem cells in muscle[J]. *Cell*, 2007, 129(5): 999-1010.
- [20] BACHMAN J F, CHAKKALAKAL J V. Satellite cells in the growth and maintenance of muscle[J]. *Curr Top Dev Biol*, 2024, 158: 1-14.
- [21] COLLINS B C, KARDON G. It takes all kinds: heterogeneity among satellite cells and fibro-adipogenic progenitors during skeletal muscle regeneration [J]. *Development*, 2021, 148(21): dev199861.
- [22] PIETROSEMOLI N, MELLA S, YENNEK S, et al. Comparison of multiple transcriptomes exposes unified and divergent features of quiescent and activated skeletal muscle stem cells[J]. *Skeletal Muscle*, 2017, 7(1): 28.
- [23] SU Y, YU Y Y, LIU C C, et al. Fate decision of satellite cell differentiation and self-renewal by miR-31-IL34 axis[J]. *Cell Death Differ*, 2020, 27(3): 949-965.
- [24] SONG Z W, JIN C L, YE M, et al. Lysine inhibits apoptosis in satellite cells to govern skeletal muscle growth *via* the JAK2-STAT3 pathway[J]. *Food Funct*, 2020, 11(5): 3941-3951.